1 # Skilful probabilistic predictions of UK flood
2 # risk months ahead using a large-sample
3 # machine learning model trained on
4 # multimodel ensemble climate forecasts

5 Simon Moulds[1,2*], Louise Slater[2], Louise Arnal[3], Andy Wood[4,5]

6 [1] School of GeoSciences, University of Edinburgh, UK [@simmoulds].

7 [2] School of Geography and the Environment, University of Oxford, UK.

8 [3] Ouranos, Montreal, Canada

9 [4] Climate and Global Dynamics, National Center for Atmospheric Research, Boulder, CO,
10 USA

11 [5] Department of Civil and Environmental Engineering, Colorado School of Mines, Golden,
12 CO, USA

13 * *Corresponding author email*: simon.moulds@ed.ac.uk

16

Abstract

Seasonal streamflow forecasts are an important component of flood risk management. Hybrid forecasting methods that predict seasonal streamflow using machine learning models driven by climate model outputs are currently underexplored, yet have some important advantages over traditional approaches using hydrological models. Here we develop a hybrid subseasonal to seasonal streamflow forecasting system to predict the monthly maximum daily streamflow up to four months ahead. We train a quantile regression forest model on dynamical precipitation and temperature forecasts from a multimodel ensemble of 196 members (eight seasonal climate forecast models) from the Copernicus Climate Change Service (C3S) to produce probabilistic hindcasts for 579 stations across the UK for the period 2004-2016, with up to four months lead time. We show that the large-sample (multi-site) ML model trained on pooled catchment data together with static catchment attributes is narrowly but significantly more skilful compared to single-site ML models trained on data from each catchment individually. Considering all initialization months, 60% of stations show positive skill (CRPSS>0) relative to climatological reference forecasts in the first month after initialization. This falls to 41% in the second month, 38% in the third month and 33% in the fourth month.

1 Introduction

Reliable streamflow forecasts weeks to months ahead are vital for managing the impacts of hydrological variability and extremes. Dynamical subseasonal to seasonal (S2S) streamflow forecasts are commonly produced by forcing a conceptual or physics-based hydrological model with the outputs of dynamical seasonal forecasts from climate models, and may also include a subsequent statistical or machine learning post-processing step. This may be achieved either directly or indirectly – e.g., by using dynamical climate prediction information as direct inputs to the hydrological model, or by using the dynamic predictions or empirical information as conditioning factors in a statistical weather generation scheme to create the model's input meteorological forecasts. These systems represent the current standard in S2S streamflow forecasting, underpinning flood forecasting services in Europe (Arheimer et al., 2020; Arnal et al., 2018), the USA (Demargne et al., 2014), Australia (Bennett et al., 2017), and globally (Emerton et al., 2018).

2

47   The chaotic nature of the atmosphere places a time limit of around 14 days on the

48   predictability of weather from initial atmospheric circulation conditions, although this limit

49   may vary from less than a week to nearly three weeks depending on local climate features

50   and the current weather regime. S2S hydro-meteorological forecasts therefore rely on

51   relatively slowly-varying aspects of the climate system that are more predictable beyond

52   weather time scales, including initial hydro-meteorological conditions and large-scale

53   climate variability modes (Doblas-Reyes et al., 2013; Emerton et al., 2018). While the skill

54   of seasonal climate forecasts is relatively low in the extra-tropics compared to other parts of

55   the world (Doblas-Reyes et al., 2013), recent progress in forecasting European climate has

56   resulted in skilful seasonal climate forecasts that support various climate services (e.g.

57   Arheimer et al., 2020). For example, the European Flood Awareness System (EFAS) is at the

58   forefront of operational streamflow forecasting in Europe, providing a pan-European service

59   that aims to support preparatory action before major floods. The seasonal component of

60   EFAS uses precipitation, temperature and evaporation from the ECMWF System 5 (SEAS5)

61   seasonal prediction system to drive LISFLOOD, a physics-based distributed hydrological

62   model that estimates hydrological states and fluxes with a daily time step (Arnal et al.,

63   2018). Operationally, EFAS produces seasonal streamflow outlooks for Europe at the

64   beginning of each month up to seven months ahead. Previous work using this setup

65   suggests that skilful forecasts may be obtained for lead times up to one month ahead, but

66   that skill decreases gradually thereafter (Arnal et al., 2018).

67   The conceptual and physics-based hydrological models used operationally are

68   computationally intensive relative to data-driven (statistical, empirical, machine learning)

69   approaches. Spatial downscaling and bias correction of meteorological forecasts are needed

70   to bridge the gap between the relatively coarse spatial scale of S2S climate prediction

71   systems and the finer resolution inputs needed by hydrological models, introducing a layer

72   of methodological uncertainty to the process-based seasonal hydrologic forecasting process.

73   The hydrological forecast outputs may then require further bias-correction before they can

74   be used (Yuan et al., 2015). In contrast, hybrid methods for seasonal streamflow forecasting

75   overcome many of the shortcomings of dynamical approaches (Slater et al. 2023). Instead of

76   using the downscaled outputs of dynamical seasonal prediction systems to drive a

77   hydrological model, hybrid methods use dynamical climate predictions to drive statistical or

78   machine-learning models to directly predict the target variables of interest – e.g. streamflow

79   quantiles or flood frequency. The dynamical climate predictions provide valuable

80   information on large-scale climate patterns and atmospheric conditions, while the statistical

81   or machine-learning models offer the ability to capture complex nonlinear relationships

82   related to streamflow behaviour. Such hybrid approaches follow from similar concepts used

83   in empirical S2S hydrologic prediction, in which observed climate system variables,

84   reanalyses or indices (but not dynamical climate forecasts) are used in statistical schemes to

85   predict streamflow directly (e.g. Mendoza et al., 2017; Regonda et al., 2006).

86   By combining the strengths of both dynamical and statistical approaches, hybrid

87   methods have shown promise for improving seasonal streamflow predictions. For example,

88   Tian et al. (2022) developed a hybrid framework that skilfully predicted month-ahead

89   reservoir inflows in two US watersheds (in Colorado and Alabama) using an ML model driven

90   by seasonal climate forecasts, observed large-scale climate indices and satellite-based

91   estimates of antecedent conditions. In Europe, Hauswirth et al. (2023) showed that a single-

92   site hybrid seasonal forecasting system could skilfully predict surface water level up to three

93   months ahead using ML models driven by climate and hydrological inputs from SEAS5.

94   Hybrid methods are unconstrained by the need to conserve the water balance and can

95   implicitly handle biases in the climate data (Slater et al., 2023). Further, they are able to

96   exploit relationships between variables at different spatial and temporal resolutions and

97   spatial extents – e.g. relating daily local streamflow quantiles to monthly climate inputs or

98   large-scale climate patterns (Moulds et al., 2023; Tian et al., 2022).

99   Previous work using observed data for hydrological simulation has shown that ML

100   models work best when trained on data from multiple catchments (Nearing et al., 2021).

101   While much of the recent literature on this topic focuses on deep learning architectures

102   (e.g. Kratzert et al., 2019), similar results have been found for tree-based models (e.g. Gauch

103   et al., 2021). Large-sample (or multi-site) approaches allow the models to learn relationships

104   from a large envelope of hydrological variability that encompasses a broad spectrum of

105   catchment characteristics, which they can use effectively to make predictions in individual

106   catchments (e.g. Lees et al., 2021; Lees et al., 2022). However, the potential added value of

107   a large-sample approach has not yet been evaluated for seasonal flood prediction using ML

108   models trained on climate forecasts. Addressing this gap is necessary because seasonal

109   climate forecasts are typically highly uncertain, at levels of skill near a minimal threshold of

110   uncertainty. The sample size of available records for training hydrological forecast models is

111   much smaller at sub-seasonal to seasonal scales than at short to medium range scales. Thus,

112   new methods that pool forecasts over space as well as time may be a promising strategy to

113   extract greater forecast signal from small-sample noise.

114   Here we develop and test a hybrid forecasting system to predict the monthly

115   maximum daily flow values (Q_{max}) at lead times of up to four months for 579 catchments in

116   the UK. The maximum probable flow in each month is an indicator of flood risk, though it

117   does not predict the exact timing or volume of a future flood event. We train a large-sample

118   machine learning model to predict Q_{max} using seasonal forecasts of precipitation and

119   temperature from the Copernicus Climate Change (C3S) multimodel ensemble alongside

120   antecedent conditions and catchment characteristics. We focus on the monthly maximum

121   daily streamflow rather than other common S2S hydrologic predictands (such as monthly or

122   seasonal average flow) because it serves as an indicator of future flood hazards at S2S lead

123   times while also presenting a significant challenge, as individual flood events (timing and

124   magnitude) cannot be skilfully predicted beyond weather time scales. We address two main

125   research questions: (i) How skilfully can the monthly maximum daily flow be predicted

126   several months ahead using uncorrected monthly dynamical climate forecasts and

127   antecedent conditions? (ii) To what extent can the skill of S2S streamflow predictions be

128   improved at individual sites by developing a large-sample machine learning model that

129   leverages static catchment attributes from a large collection of catchments to learn the

130   hydrological behaviour at individual sites?

2 Materials and methods

2.1 Data

2.1.1 Streamflow

For the prediction target and observational validation dataset we used daily streamflow observations for Great Britain from the National River Flow Archive (NRFA, 2024). We first selected stations that had streamflow records between 1994 and 2016 to match the hindcast period of the climate models, before discarding stations with less than 95% data availability in any given year. We also discarded any stations that were not included in the CAMELS-GB dataset (Coxon et al., 2020), leaving a total of 579 stations. We computed specific discharge (mm day^{-1}) by dividing the daily streamflow values by the catchment area, then calculated the monthly maximum daily specific discharge for all months and stations.

2.1.2 Climate (re)forecasts

Monthly predictions of precipitation and temperature were obtained from the Copernicus Climate Change (C3S) multimodel seasonal forecasting system. We took seasonal reforecasts ("hindcasts") of precipitation and temperature for the period 1994-2016 from eight seasonal prediction systems, resulting in a large multimodel ensemble of 196 members (Table S1). We computed the multimodel ensemble mean values of precipitation and temperature. We found that including quantiles (0.05, 0.25, 0.5, 0.75, 0.95) drawn from the precipitation and temperature ensemble as additional covariates alongside the mean values in the ML models did not improve skill (results not shown). We computed the climate inputs for each catchment by taking the area-weighted average monthly value for each variable. All C3S forecasting systems are assigned a nominal start date of the first day of each month such that no members are initialized using observations later than this date, although the initialization method varies across the individual systems. Hereafter we refer to the predictions for the month immediately following initialization as having a lead time of zero (e.g. for a forecast initialized on August 1st, the zeroth lead time prediction covers August 1-31st). The C3S forecasting system predicts climate up to a minimum of 6 months ahead, but we focus on the first 4 months following initialization as

160 we are unlikely to observe substantial skill for monthly predictands thereafter (e.g. Arnal et

161 al., 2018; Harrigan et al., 2018).

162 **2.1.3 Antecedent catchment conditions**

163   We used antecedent mean monthly streamflow as a proxy indicator of initial

164 catchment soil moisture conditions, an important driver of seasonal hydrologic predictability

165 (Arnal et al., 2018; Bierkens & Van Beek, 2009). We used the monthly mean specific

166 discharge in the three months prior to the forecast initialization to create three predictor

167 variables describing the mean specific discharge over one month, two months and three

168 months prior to the nominal forecast initialization date, respectively. We also included

169 estimates of antecedent precipitation using ERA5 reanalysis data, creating variables to

170 represent the average precipitation over one month, two months and three months prior to

171 the initialization time. Antecedent precipitation and streamflow are both employed as

172 proxies for hydrologic initial conditions and are likely to exhibit some degree of collinearity.

173 However, as random forests are relatively robust to multicollinearity, we chose to retain

174 both predictors in the model.

175 **2.1.4 Catchment attributes**

176   Large-sample ML models trained on data from hundreds of stream gauges

177 simultaneously can benefit from additional information about spatial variability in

178 catchment characteristics relative to single-site models (e.g. Lees et al., 2021, Slater et al.,

179 2024). Here we included static catchment descriptors from the CAMELS-GB dataset (Table

180 S3; Coxon et al., 2020) in our ML model. We also tried including streamflow signatures that

181 describe the hydrologic behaviour of each catchment, including the baseflow index, slope of

182 the flow duration curve, the 5th and 95th percentile of daily streamflow, and the mean daily

183 streamflow. These were computed using data up to the start of the test period (2004) of our

184 hybrid models, to prevent data leakage (i.e., the situation where a statistical or ML model is

185 inadvertently trained on the same data it will later be tested on). However, although the

186 signature predictors assumed high importance in the QRF model, they did not increase Q_{max}

187 forecasting skill, suggesting that the model can learn these hydrological characteristics from

188   the static catchment attributes alone. We therefore left out the streamflow signatures from

189   the final multi-site model.

2.2 Methods

191   We predict the monthly maximum daily streamflow (Q_{max}) using both dynamic and

192   static predictor variables. Most large-sample ML approaches for hydrologic prediction

193   employ Long Short Term Memory models (LSTMs), which are well-suited for sequential

194   modelling at daily timesteps. However, in this study, we employ quantile regression forests

195   (QRF; Meinshausen, 2006), a nonparametric ensemble method that is well-suited for

196   working with single monthly aggregated forecasts from C3S. QRFs extend traditional

197   random forests (Breiman, 2001) by estimating conditional quantiles of the response

198   variable, enabling probabilistic predictions. Like random forests, QRFs are adept at

199   exploiting nonlinear relationships between dependent and independent variables and

200   require relatively little tuning because their performance is less sensitive to the values of

201   hyperparameters compared to many other ML methods (Tyralis et al., 2019). QRFs can also

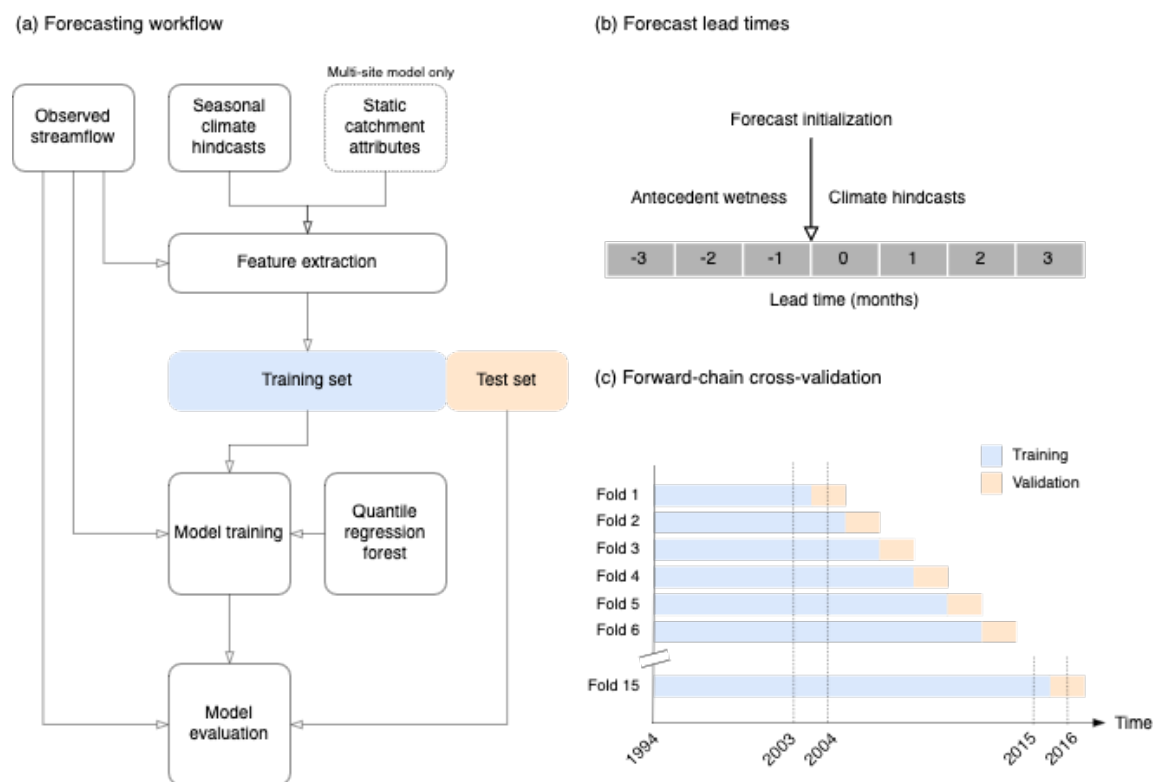202   be interrogated to establish the relative importance of predictor variables.

203

2.2.1 Model training

We train the model directly on the dynamical S2S forecast outputs to avoid introducing additional uncertainty due to post-processing (Figure 1a). Like other forms of regression, the ML model implicitly performs bias correction by relating the raw climate inputs to observed streamflow (e.g. Slater et al. 2023; Slater and Villarini 2018). We compared three model structures to predict Q_{max} in each catchment (Table 1). First, we trained QRF models on each streamflow time series independently, giving a site-specific model for every catchment. We compared the single-site models with a multi-site QRF model that was trained on all (n=579) available streamflow time series data at once. To assess the extent to which the multi-site model learns from catchment attributes, we also include a multi-site model with the catchment ID as the only static attribute. Owing to the inherent robustness of QRF to potentially irrelevant predictors, whereby unimportant features are automatically downweighted, we do not perform predictor variable selection or screening.

Table 1: Formulation of the three ML models used in the analysis. Precipitation and temperature are the monthly ensemble mean values from the C3S multimodel system. Antecedent precipitation is the forecasted precipitation from the month prior to the target month, with lead time varying between 1 and 3 months (i.e. to make a prediction in lead time 4 the antecedent precipitation would be taken from lead time 3). Antecedent streamflow is the mean daily observed streamflow prior to the forecast initialization. Catchment attributes are listed in Table S1.

Model name	Configuration	Model description
Single-site	Single-site	Precipitation, temperature, antecedent streamflow and precipitation
Multi-site with ID	Multi-site	As for single-site model, plus catchment ID
Multi-site with attributes	Multi-site	As for single-site model, plus 15 static catchment attributes

230   In both single-site and multi-site approaches, a separate QRF model is trained for

231   each lead time using all months from the training period. This is because the biases in the

232   climate forecasts often change over time from initialization, so a model trained on climate

233   forecasts with a lead time of one month would be unsuitable to make predictions using

234   climate forecasts with a lead time of two months. We note that a similar approach is used

235   for bias correcting seasonal climate forecasts (Crochemore et al., 2016). Another possibility

236   would be to train a model on all lead times at once, with the lead time itself included as a

237   categorical variable. We tried this but found that it degraded predictive skill. Thus, for each

238   training period we obtain four models, trained on climate predictions with lead times of

239   one, two, three and four months ahead, respectively (Figure 1b). Dataset stratification

240   choices are important in S2S prediction because predictability and prediction system biases

241   typically vary seasonally and with lead time. There are strong geophysical reasons to tailor a

242   statistical or empirical model using both factors, but each stratification dimension reduces

243   the sample size available for training and testing, thus a trade-off is often adopted (e.g.

244   Lehner et al., 2017). Here we do not stratify by initialization date (i.e., month). We

245   construct an ensemble forecast by using the QRF model to predict the conditional quantiles

246   of Q_{max} corresponding to probabilities between 0.01 and 0.99, with an interval of 0.02.

247   We use a forward-chain cross-validation approach whereby the models are trained on

248   reforecasts from the previous n years and tested on the current year (Figure 1c). For

249   example, to predict all months in 2004, the first training period was taken as January 1994

250   to December 2003. For 2005, we then extended the training period by one year to

251   December 2004, and continued adding one year until 2016, the final year in the test period,

252   at which point the training period for the QRF models was January 1994 to December 2015.

253   The climate predictors consisted of the multimodel ensemble mean of monthly precipitation

254   and temperature (Table S1). We did not include a separate validation dataset (i.e., in a

255   train/validate/test framework) because we found there was limited benefit to be gained

256   from tuning the hyperparameters of the QRF model. The forward-chain cross-validation

257   approach means that the model was retrained each year using data up to the previous year.

258   The overall test results combine the test results for the individual years. This ensures the

259   model is never tested on data it has been exposed to during training.

260

261 2.2.2 Forecast evaluation

262   We evaluated predictive skill using the continuous ranked probability score (CRPS)
263 and associated skill score (CRPSS), common metrics for ensemble forecast evaluation. The
264 CRPS represents the error between the forecast and observed cumulative distribution
265 functions (Wilks, 2019). It ranges between zero and positive infinity and is negatively
266 oriented (i.e. smaller values are better), similar in concept to other common error terms
267 (e.g., mean absolute error). We evaluated our forecasts against an observation-based
268 ensemble climatological forecast consisting of the observed monthly maximum daily
269 streamflow values from the previous 20 years (e.g. Hauswirth et al., 2023), as well as EFAS
270 seasonal hindcasts. We used the CRPSS to evaluate the probabilistic skill of our ML forecasts
271 relative to the reference ensemble climatology. The CRPSS ranges between negative infinity
272 and 1, where 1 indicates perfect skill and 0 or below indicates no skill compared to the
273 reference forecast. We computed the CRPS of the forecast and reference for each month in
274 the test period (2004-2016) and took the mean across individual months to compute the
275 CRPSS.

276   We complemented the CRPS (CRPSS) with the anomaly correlation coefficient (ACC)
277 and reliability index (RI) (Renard et al., 2010). The ACC varies between -1 and 1, with a score
278 of 1 representing perfect correlation between observed and forecast streamflow values. The
279 RI is a probabilistic measure of the extent to which the forecast ensemble spread represents
280 the uncertainty in observations. It varies between 0 and 1, with 1 denoting a perfectly
281 reliable forecast. Like the CRPSS, we calculate the ACC and RI for every month and lead time
282 separately. Lastly, we assessed the relative importance of the predictor variables using the
283 Gini index, which measures the importance of individual variables in tree-based ML models.
284 Specifically, the Gini index quantifies the extent to which a variable contributes to making
285 homogeneous groups, where outcomes are similar and predictions are more reliable, while
286 reducing impurity, indicating mixed groups with less predictable outcomes.

287

288 **3 Results**

289   The multi-site model with catchment attributes significantly outperforms the multi-

290   site model with the catchment ID alone (Figure 2a). This suggests that including static

291   catchment attributes enables the model to better reproduce the hydrologic behaviour of

292   different catchments, aligning with previous research for the UK on ML applied to daily

293   streamflow simulation using observed climate inputs (e.g. Lees et al., 2021; Lees et al.,

294   2022), and with findings on the performance of ML models for prediction in ungauged

295   basins (Kratzert et al. 2019). Considering the skill scores for each lead time and combining all

296   initialization months, the multi-site model with catchment attributes narrowly but

297   significantly outperforms the single-site models at lead times of one to three months, with a

298   similar average performance between the multi-site and single-site model for the zeroth

299   lead time (Figure 2b). However, the relative performance of the multi-site model with

300   attributes and the single-site model varies by forecast month and lead time (Figure 3). For

301   the zeroth lead time, the multi-site model tends to outperform the single-site model in the

302   months where the highest skill is observed (i.e. December, January, June, July).
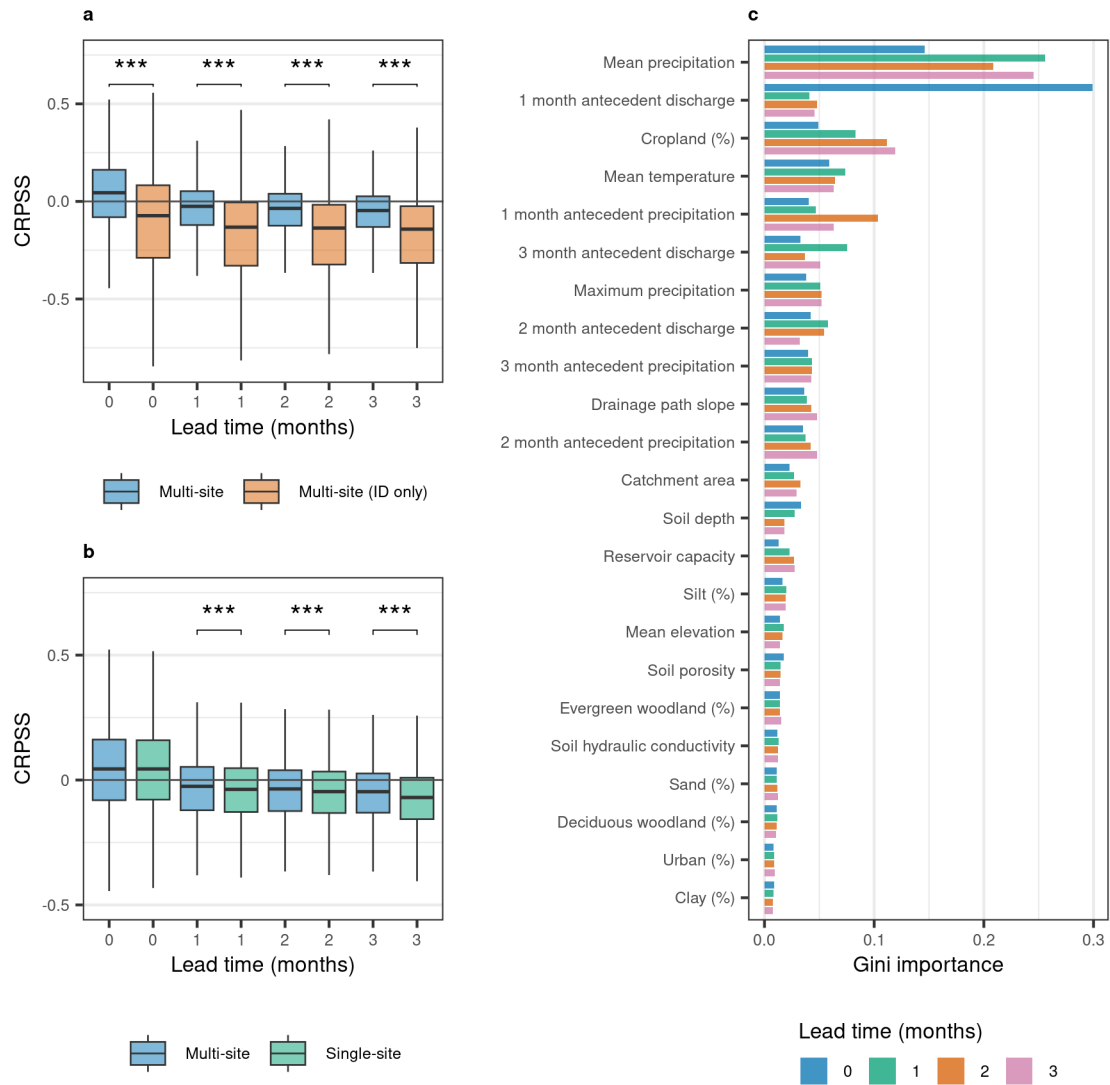
303

Figure 2: Analysis of model performance. **a.** Comparison of CRPSS for all months for multi-site models with catchment attributes and with the catchment ID only. We used a two-sided Wilcoxon signed rank test to assess whether differences in skill scores between the models were significant (*** = p < 0.001, ** = p < 0.01, * = p < 0.05). **b.** Comparison of single-site model with multi-site model with catchment attributes. **c.** Relative importance of predictor variables in the multi-site model with catchment attributes for each lead time. Time-varying predictors are marked with an asterisk (e.g. *Mean precipitation).

We used the Gini index to assess the importance of each predictor variable to the multi-site model with catchment attributes at each lead time (Figure 2c). Monthly precipitation forecasts have high importance across lead times, while mean temperature forecasts have moderate importance. We also included antecedent conditions from observed streamflow and forecast precipitation. Antecedent streamflow is the most important variable at one-month lead time but decreases with importance at later lead

324   times. This is because we are limited to providing antecedent conditions prior to forecast

325   initialization, which has decreasing relevance as the lead time increases, reflecting our

326   general understanding of the influence of initial versus boundary conditions in S2S

327   hydrologic forecasting (e.g. Wood et al., 2016).

328   We assessed skill by computing the monthly CRPSS using a climatological prediction

329   as a reference. We find that there is significant variability in skill during the different months

330   of the year (Figure 5a), especially at shorter lead times. For lead time 0, we observed the

331   highest skill in extended winter (DJFM) and late summer (JJAS), with lower skill during spring

332   and autumn. This is a positive result because in the UK high river flows are usually seen

333   during the winter months. In December and July more than 80% of stations have positive

334   skill in lead time 0 (Table 2). In most months, the skill decreases sharply over time, whereas

335   for other months (e.g. March) the skill remains relatively consistent as lead time increases.

336   The variation in skill likely reflects the varying importance of antecedent conditions during

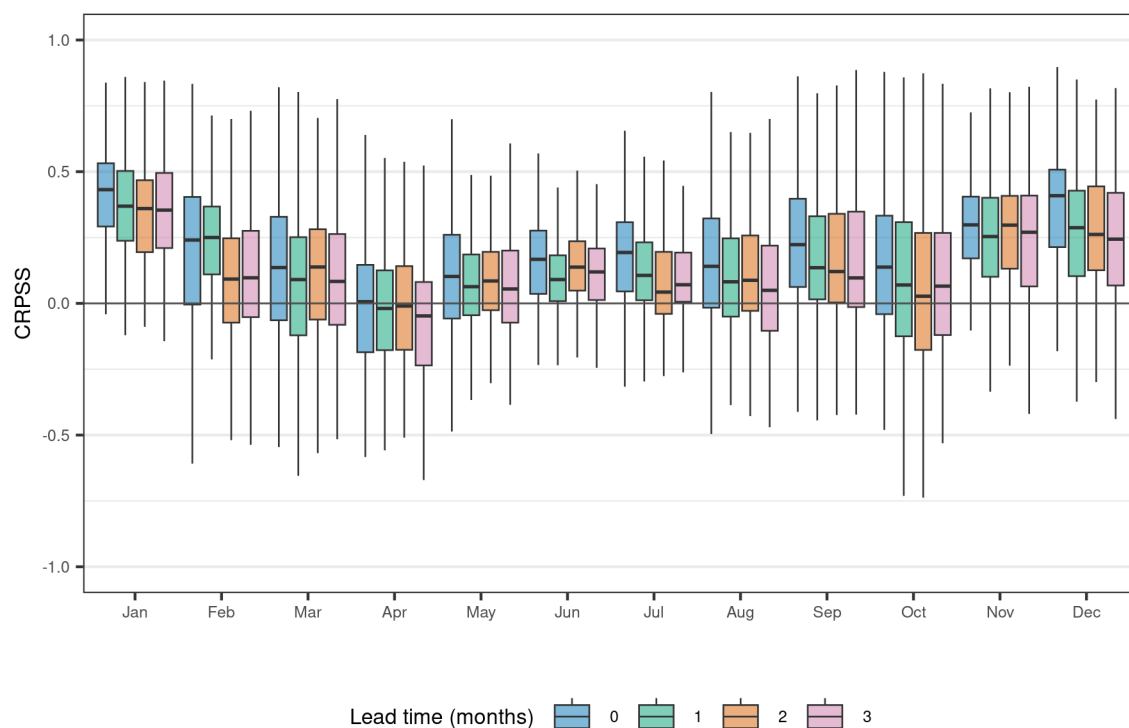337   the year, as well as the varying skill of the climate forecasts.

338

339   **Figure 4:** Continuous rank probability skill score of the multi-site model with catchment

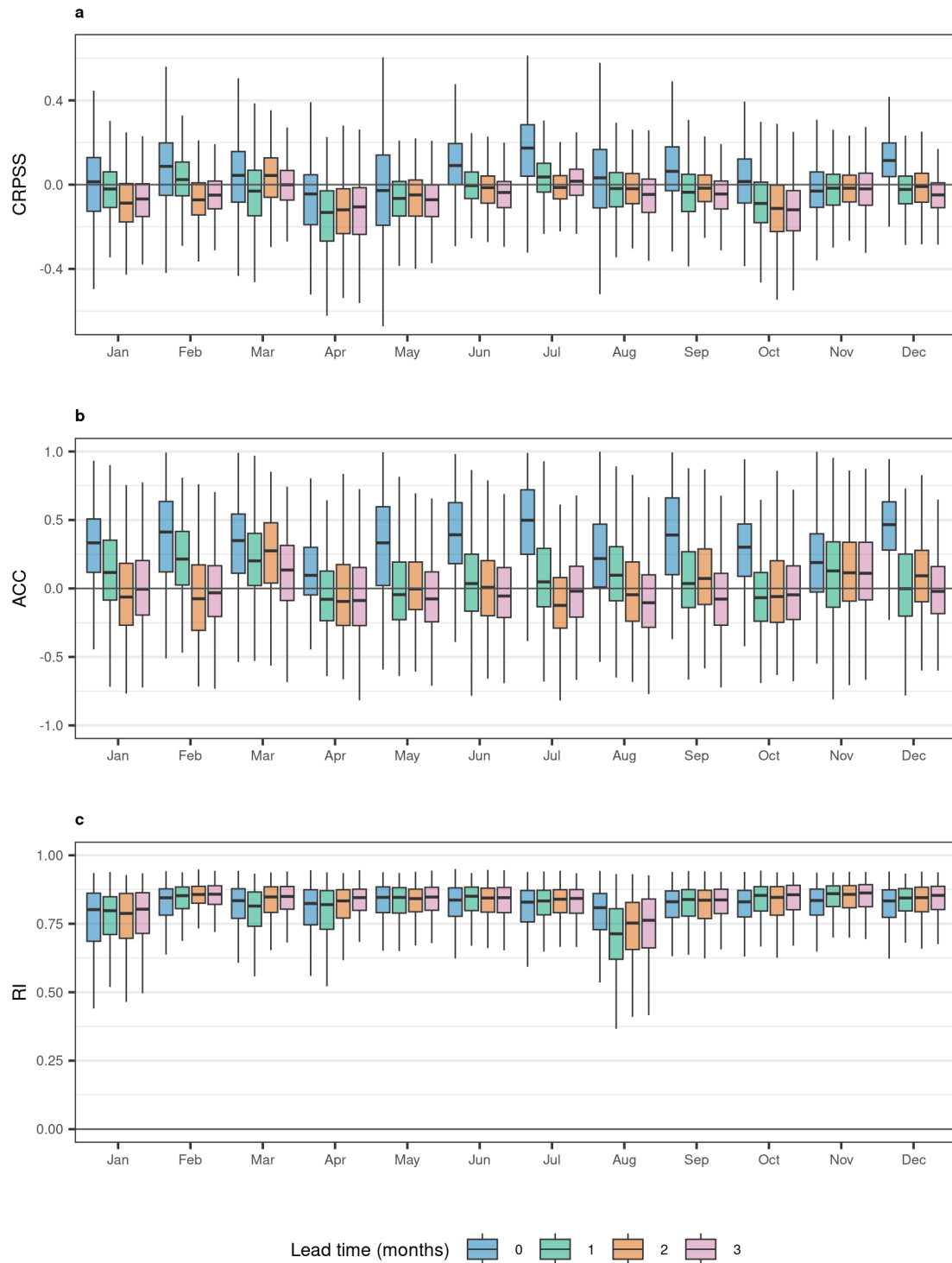340   attributes using bias-corrected EFAS seasonal hindcasts as a benchmark.

341

a

b

c

Lead time (months) 0 1 2 3

342

343 **Figure 5:** Performance assessment of the multi-site model with catchment attributes for

344 each forecast month and lead time, using an ensemble climatological forecast as the

345 reference. **a.** Continuous ranked probability skill score (CRPSS). We use climatological

346 forecast as the reference forecast, which is computed separately for each test year in the

347 simulation. **b.** Anomaly correlation coefficient (ACC). **c.** Reliability index (RI). The four lead

348 times are shown with different colours.

349 As with the CRPSS, the ACC varies by forecast month and lead time (Figure 5b), with

350 the monthly variability in ACC following a similar pattern to that of the CRPSS. At lead time

351 0, the ACC is positive in >75% of stations across all months. During lead time 1, the ACC is

352 positive in >50% of stations in all months except April, May, and October. Compared to the

353 CRPSS and the ACC, the RI is more consistent across months and lead times (Figure 5c).

354 Overall, our ensemble hindcasts have high reliability, with the mean RI across all stations

355 exceeding 0.8 in all months except August.

356 We also compared our results to monthly Q_{max} drawn from daily EFAS seasonal

357 predictions for a subset of the stations included in this study (n=188) that overlapped with

358 the EFAS reference dataset. We bias corrected the EFAS outputs using a quantile mapping

359 approach employing an empirical cumulative distribution function so that they could be

360 directly compared with observations. As EFAS produces daily streamflow estimates we took

361 the maximum daily streamflow prediction from each month and used this value as the

362 reference forecast to estimate CRPSS. Our results are skilful compared to EFAS (Figure 4),

363 and this high relative skill, coupled with the general lack of positive skill of the QRF forecast

364 for lead times of 1-3 months compared to a climatological reference, indicates that the EFAS

365 predictions were poorer than expected as a benchmark for this monthly extreme target

366 variable. We note that our model is specifically trained to predict Q_{max}, while EFAS seasonal

367 forecasts are developed for more general purposes, such as supporting tercile probability

368 forecasts for monthly or seasonal mean conditions, a common S2S hydrological product

369 (e.g. Arnal et al., 2018).

370 **Table 2:** Percentage of stations (n=579) that are skilful (CRPSS>0) compared to

371 climatological reference forecast at each lead time and forecast month for the multi-site

372 model with catchment attributes.

Forecast month	Lead time			
	0	1	2	3
January	51.7	42.2	25.3	26.3
February	66.1	59.2	28.0	29.4

March	58.8	42.2	62.3	50
April	38.4	19.2	22.0	20.8
May	46.0	29.8	33.6	24.4
June	76.1	48.3	44.3	31.0
July	81.1	64.5	41.7	59.3
August	56.4	44.3	42.6	33.6
September	67.1	38.2	43.8	31.7
October	53.8	26.6	23.5	18.9
November	40.1	41.3	42.2	42.2
December	83.4	40.0	45.5	28.2

373   We examined the spatial variability in model skill by averaging the monthly skill
374   scores for the multi-site model (with catchment attributes) within each season (Figure 6). At
375   lead time 0 we observe skill across much of the UK, while at later lead times, skilful
376   catchments tend to cluster in southern England. This could be related to the presence of
377   relatively slower responding catchments with greater subsurface storage in the south-
378   eastern UK. However, we found relatively weak correlation between ACC and the baseflow
379   index (R=0.33, 0.31, 0.27, 0.25 for the four lead times). We observe a tendency for the QRF
380   models to underestimate the observed Q_{max}, especially the more extreme values (Figure 7).
381   The underestimation is more pronounced as lead time increases, likely due to greater noise
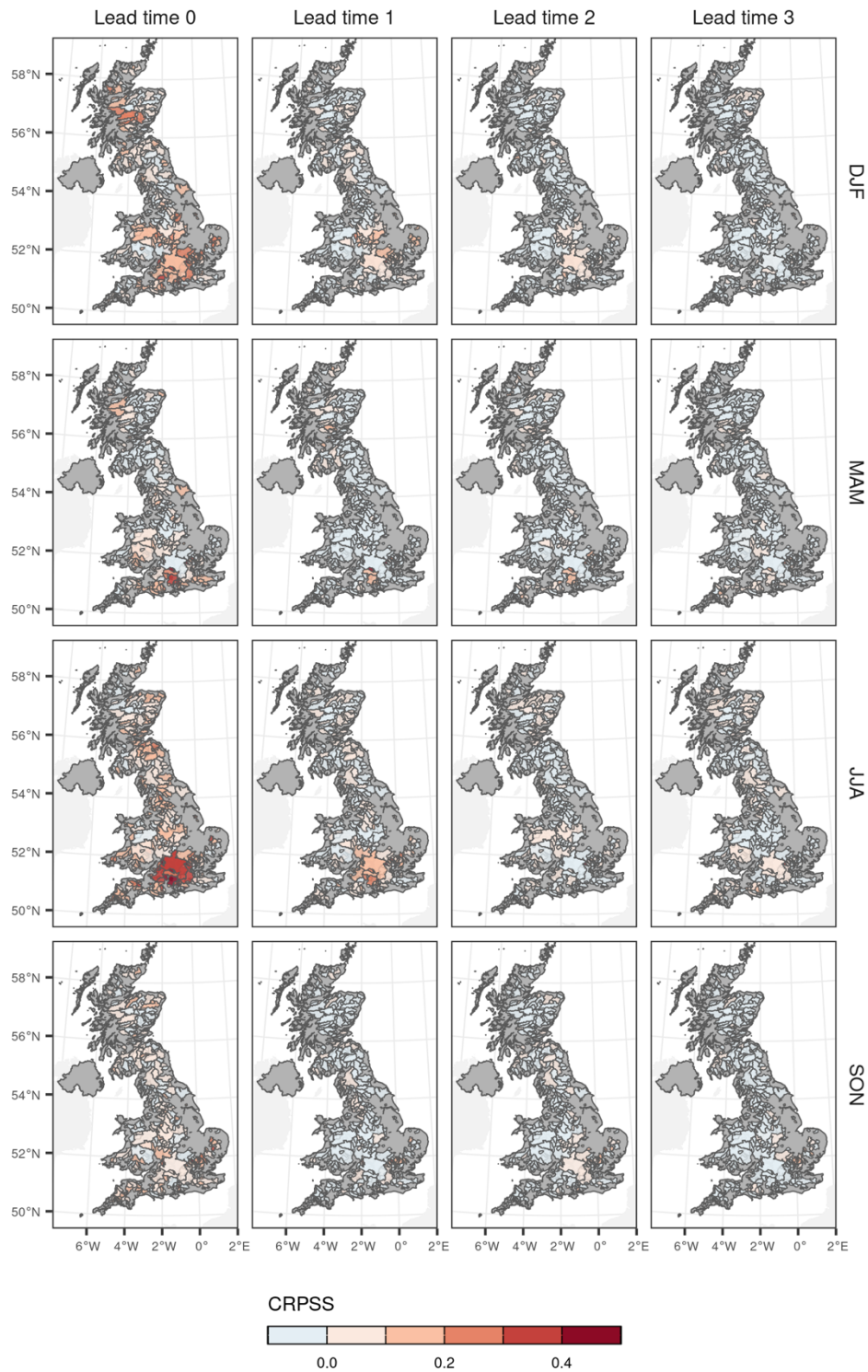382   in the seasonal climate forecasts at longer lead times.

384 **Figure 6:** Average seasonal skill compared to climatological reference forecast in every

385 catchment by lead time. We calculate the CRPSS per month and catchment, then compute

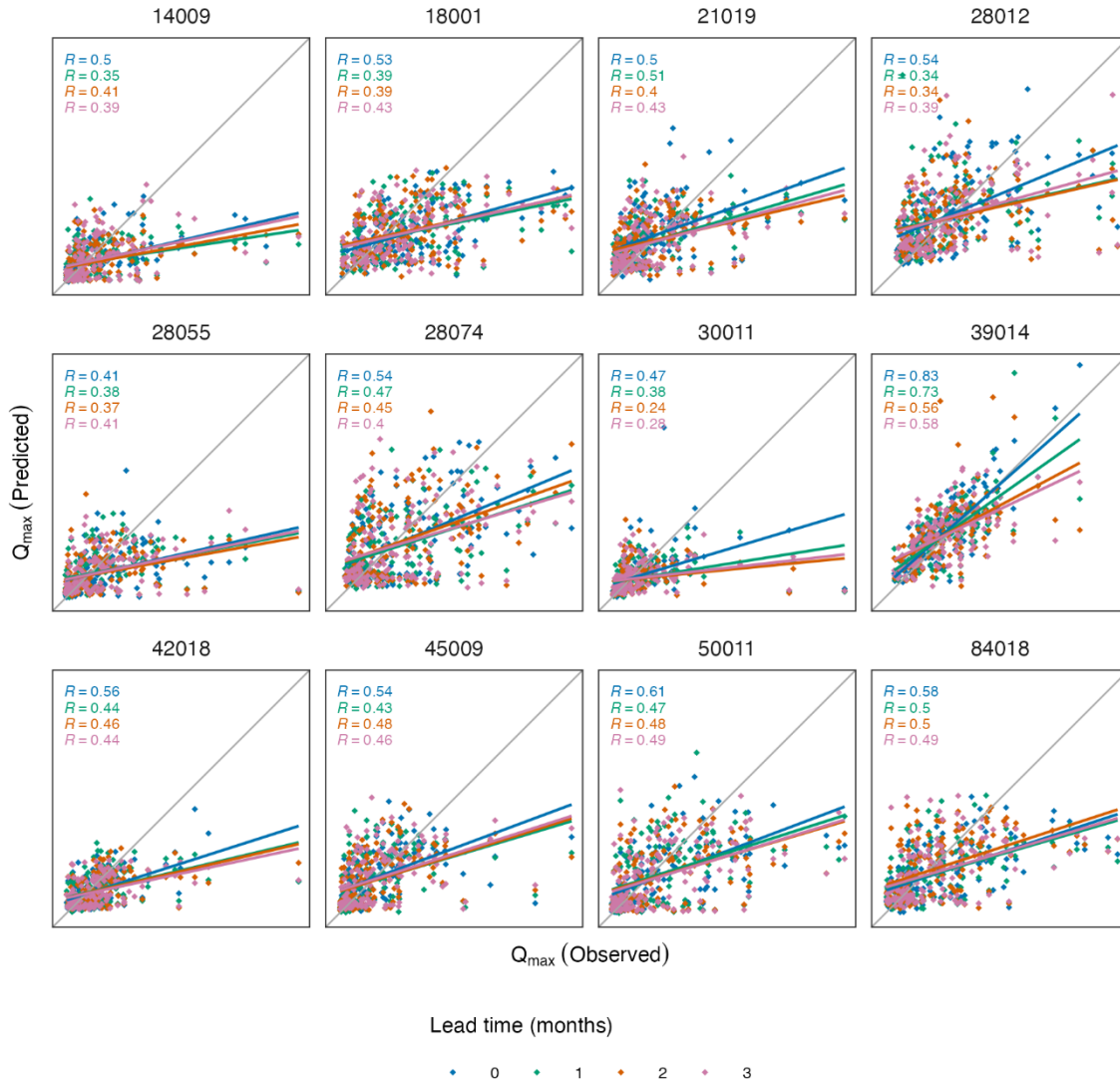386 the seasonal average (DJF, MAM, JJA, SON).

Figure 7: Comparison of observed and predicted Q_{max} across all months for 12 randomly
selected catchments, by lead time.

4 Discussion

We developed a hybrid forecasting approach for UK flood risk prediction at
subseasonal-to-seasonal time scales using a large multimodel ensemble of climate
predictions. Addressing our first research question, we found that S2S flood predictions are
generally skilful (CRPSS>0) up to 1 month following initialization, but skill declines
thereafter. However, 90 stations out of 579 retained positive skill in at least three months of
the year for all four lead times. Across all initialization times, 60% of stations show positive
skill compared to the climatological benchmark in the first month after initialization. This

20

proportion drops to 41% in the second month, 38% in the third month and 33% in the fourth month. The level of skill varies within the year, with some months generally more skilful than others. The seasonal variation in skill is likely due to a combination of varying climate predictability and the varying importance of antecedent conditions to flood magnitude and frequency during the year. The underlying seasonal forecasts of precipitation and temperature are also most skilful at shorter lead times, although they retain some information at longer lead times.

Our work provides guidance on how to build hybrid streamflow prediction systems that combine ML with dynamical model forecasts. With respect to our second research question, we found that a large-sample ML model trained on data from all catchments at once tends to outperform single-site model forecasts across all lead times. This results aligns with previous research on ML-based hydrological modelling, which revealed the benefit of a larger training dataset in large-sample models relative to single-site approaches (e.g. Kratzert et al., 2019). However, our work specifically considers forecasting months ahead, whereas previous work only studied out-of-sample simulation or short-term prediction using observed meteorological or weather forecast inputs. The large-sample approach enables ML models to combine information across time and space into a single model that is trained to discriminate a range of hydrological behaviours. The inclusion of static catchment attributes enables such models to learn the different rainfall-runoff behaviours across many catchments. This is especially important when using ML to predict extremes when training data are limited in time, as it means multi-site models remain realistic over a larger range of conditions than single-site models.

Hybrid prediction systems require training and testing partitions to evaluate model performance, and different approaches exist to do this. Here we implemented a forward-chain cross validation approach such that the model is never trained on data more recent than the test partition. This reproduces an operational setup as far as possible, where the model is never exposed to information from the future. However, one limitation of this approach for hindcast studies is that the relatively short hindcast period of the C3S multimodel ensemble (i.e. 1994-2016) means the smallest training partition may contain as few as 10 years of monthly data. Nevertheless, during model development we found that increasing the length of the training period – by focusing on the predictions from the SEAS5

429   system, which has an extended hindcast period of 1981-2016 – did not significantly enhance

430   the performance of the QRF models (results not shown). Moreover, using a multi-site

431   approach reduces the impact of the relatively short reforecast period by pooling data from

432   many catchments to create a much larger training dataset than is used by single-site models

433   (i.e. swapping space for time).

434   Our hybrid seasonal flood forecasts based on eight models from the C3S multimodel

435   ensemble exhibit relatively low skill, as is also the case with traditional (i.e. process-based

436   hydrological model) flood forecasting systems driven by C3S (e.g. Arnal et al., 2018). These

437   findings suggest that the primary constraint on enhanced skill lies in the seasonal climate

438   forecasts. Increasing the skill of climate forecasts is therefore a priority to achieve more

439   useful seasonal streamflow forecasts. One area for further research is to develop ways of

440   identifying ensemble members that are likely to be more skilful over a given time period.

441   Selecting members based on their ability to reproduce large-scale climate patterns such as

442   the NAO is one potential option that has proved successful in other applications (e.g.

443   Dobrynin et al., 2022; Moulds et al., 2023). Observed climate states, teleconnections and

444   indices (e.g., describing El Nino, the Southern Oscillation, and other climate modes) may be

445   similarly exploited in regions where they exert an influence on weather patterns. These

446   patterns have been deployed in empirical hydrologic forecast systems for many years, while

447   the operational outputs from climate forecast models remain a relatively less-explored

448   source of predictability in hybrid approaches.

449   **5 Conclusion**

450   Operational services for seasonal streamflow forecasts have existed for over a

451   century, offering highly skilled predictions in many parts of the world, and particularly when

452   and where predictors with long persistence are present – such as snowpack or groundwater

453   – as well as strong climate seasonality. Despite their successes, there is growing demand

454   from stakeholders for improved seasonal flow prediction skill at times and in places where it

455   has been more difficult to achieve, usually due to data limitations or hydroclimate

456   considerations.

457

458 This study illustrates that a hybrid multi-site forecasting approach trained over a large-

459 sample collections of watersheds may offer benefits for monthly to seasonal predictions of

460 streamflow. Our approach affords users significant flexibility to define target variables of

461 interest (e.g. Q_{max}). We use static catchment attributes as predictor variables to allow the

462 QRF model to learn the different relationships between hydroclimate input data and

463 monthly maximum daily streamflow, demonstrating an ability to produce skilful seasonal

464 forecasts of monthly flood risk up to four months ahead in a moderate fraction of the

465 catchments studied. The use of a multi-site ML model that is trained on data from multiple

466 catchments at once may help to alleviate the long-standing problem of small sample sizes

467 when training seasonal predictions on individual sites alone, while also enabling prediction

468 in ungauged basins. However, although the performance benefit of the multi-site model

469 over single-site models is statistically significant, the improvement is modest, suggesting

470 that the primary constraint on enhancing skill remains the quality of seasonal climate

471 forecasts themselves.

472 **Competing interests**

475 **Acknowledgements**

Data availability statement

The input data and scripts that are needed to reproduce the results of this study will be uploaded to a research data repository under an MIT license upon acceptance for publication. They can be made available to reviewers upon request.

References

Arheimer, B., Pimentel, R., Isberg, K., Crochemore, L., Andersson, J. C. M., Hasan, A., & Pineda, L. (2020). Global catchment modelling using World-Wide HYPE (WWH), open data, and stepwise parameter estimation. *Hydrology and Earth System Sciences*, *24*(2), 535–559. https://doi.org/10.5194/hess-24-535-2020

Arnal, L., Cloke, H. L., Stephens, E., Wetterhall, F., Prudhomme, C., Neumann, J., Krzeminski, B., & Pappenberger, F. (2018). Skilful seasonal forecasts of streamflow over Europe? *Hydrology and Earth System Sciences*, *22*(4), 2057–2072. https://doi.org/10.5194/hess-22-2057-2018

Bennett, J. C., Wang, Q. J., Robertson, D. E., Schepen, A., Li, M., & Michael, K. (2017). Assessment of an ensemble seasonal streamflow forecasting system for Australia. *Hydrology and Earth System Sciences*, *21*(12), 6007–6030. https://doi.org/10.5194/hess-21-6007-2017

Bierkens, M. F. P., & Van Beek, L. P. H. (2009). Seasonal Predictability of European Discharge: NAO and Hydrological Response Time. *Journal of Hydrometeorology*, *10*(4), 953–968. https://doi.org/10.1175/2009JHM1034.1

Breiman, L. (2001). Random forests. *Machine Learning*, *45*(1), 5–32.

Coxon, G., Addor, N., Bloomfield, J. P., Freer, J., Fry, M., Hannaford, J., Howden, N. J. K., Lane, R., Lewis, M., Robinson, E. L., Wagener, T., & Woods, R. (2020). CAMELS-GB: Hydrometeorological time series and landscape attributes for 671 catchments in

511   Great Britain. *Earth System Science Data*, *12*(4), 2459–2483.

512   https://doi.org/10.5194/essd-12-2459-2020

513   Crochemore, L., Ramos, M.-H., & Pappenberger, F. (2016). Bias correcting precipitation

514   forecasts to improve the skill of seasonal streamflow forecasts. *Hydrology and Earth*

515   *System Sciences*, *20*(9), 3601–3618. https://doi.org/10.5194/hess-20-3601-2016

516   Demargne, J., Wu, L., Regonda, S. K., Brown, J. D., Lee, H., He, M., Seo, D.-J., Hartman, R.,

517   Herr, H. D., Fresch, M., Schaake, J., & Zhu, Y. (2014). The Science of NOAA's

518   Operational Hydrologic Ensemble Forecast Service. *Bulletin of the American*

519   *Meteorological Society*, *95*(1), 79–98. https://doi.org/10.1175/BAMS-D-12-00081.1

520   Doblas-Reyes, F. J., García-Serrano, J., Lienert, F., Biescas, A. P., & Rodrigues, L. R. L. (2013).

521   Seasonal climate predictability and forecasting: Status and prospects. *WIREs Climate*

522   *Change*, *4*(4), 245–268. https://doi.org/10.1002/wcc.217

523   Dobrynin, M., Düsterhus, A., Fröhlich, K., Athanasiadis, P., Ruggieri, P., Müller, W. A., &

524   Baehr, J. (2022). Hidden Potential in Predicting Wintertime Temperature Anomalies

525   in the Northern Hemisphere. *Geophysical Research Letters*, *49*(20).

526   https://doi.org/10.1029/2021GL095063

527   Emerton, R., Zsoter, E., Arnal, L., Cloke, H. L., Muraro, D., Prudhomme, C., Stephens, E. M.,

528   Salamon, P., & Pappenberger, F. (2018). Developing a global operational seasonal

529   hydro-meteorological forecasting system: GloFAS-Seasonal v1.0. *Geoscientific Model*

530   *Development*, *11*(8), 3327–3346. https://doi.org/10.5194/gmd-11-3327-2018

531   Gauch, M., Mai, J., & Lin, J. (2021). The proper care and feeding of CAMELS: How limited

532   training data affects streamflow prediction. *Environmental Modelling & Software*,

533   *135*, 104926. https://doi.org/10.1016/j.envsoft.2020.104926

534   Harrigan, S., Prudhomme, C., Parry, S., Smith, K., & Tanguy, M. (2018). Benchmarking

535   ensemble streamflow prediction skill in the UK. *Hydrology and Earth System*

536   *Sciences*, *22*(3), 2023–2039. https://doi.org/10.5194/hess-22-2023-2018

537   Hauswirth, S. M., Bierkens, M. F. P., Beijk, V., & Wanders, N. (2023). The suitability of a

538   seasonal ensemble hybrid framework including data-driven approaches for

539   hydrological forecasting. *Hydrology and Earth System Sciences*, *27*(2), 501–517.

540   https://doi.org/10.5194/hess-27-501-2023

541   Kratzert, F., Klotz, D., Herrnegger, M., Sampson, A. K., Hochreiter, S., & Nearing, G. S. (2019).

542   Toward Improved Predictions in Ungauged Basins: Exploiting the Power of Machine

543   Learning. *Water Resources Research*, *55*(12), 11344–11354.

544   https://doi.org/10.1029/2019WR026065

545   Lees, T., Buechel, M., Anderson, B., Slater, L., Reece, S., Coxon, G., & Dadson, S. J. (2021).

546   Benchmarking data-driven rainfall–runoff models in Great Britain: A comparison of

547   long short-term memory (LSTM)-based models with four lumped conceptual models.

548   *Hydrology and Earth System Sciences*, *25*(10), 5517–5534.

549   https://doi.org/10.5194/hess-25-5517-2021

550   Lehner, F., Wood, A. W., Llewellyn, D., Blatchford, D. B., Goodbody, A. G., & Pappenberger,

551   F. (2017). Mitigating the Impacts of Climate Nonstationarity on Seasonal Streamflow

552   Predictability in the U.S. Southwest. *Geophysical Research Letters*, *44*(24).

553   https://doi.org/10.1002/2017GL076043

554   Meinshausen, N. (2006). Quantile Regression Forests. *Journal of Machine Learning Research*,

555   *7*, 983–999.

556   Mendoza, P. A., Wood, A. W., Clark, E., Rothwell, E., Clark, M. P., Nijssen, B., Brekke, L. D., &

557   Arnold, J. R. (2017). An intercomparison of approaches for improving operational

558   seasonal streamflow forecasts. *Hydrology and Earth System Sciences*, *21*(7), 3915–

559   3935. https://doi.org/10.5194/hess-21-3915-2017

560 Moulds, S., Slater, L. J., Dunstone, N. J., & Smith, D. M. (2023). Skillful Decadal Flood

561   Prediction. *Geophysical Research Letters*, *50*(3), e2022GL100650.

562   https://doi.org/10.1029/2022GL100650

563 Nearing, G. S., Kratzert, F., Sampson, A. K., Pelissier, C. S., Klotz, D., Frame, J. M., Prieto, C., &

564   Gupta, H. V. (2021). What Role Does Hydrological Science Play in the Age of Machine

565   Learning? *Water Resources Research*, *57*(3), e2020WR028091.

566   https://doi.org/10.1029/2020WR028091

567 Regonda, S. K., Rajagopalan, B., & Clark, M. (2006). A new method to produce categorical

568   streamflow forecasts. *Water Resources Research*, *42*(9), 2006WR004984.

569   https://doi.org/10.1029/2006WR004984

570 Renard, B., Kavetski, D., Kuczera, G., Thyer, M., & Franks, S. W. (2010). Understanding

571   predictive uncertainty in hydrologic modeling: The challenge of identifying input and

572   structural errors. *Water Resources Research*, *46*(5), 2009WR008328.

573   https://doi.org/10.1029/2009WR008328

574 Slater, L. J., Arnal, L., Boucher, M.-A., Chang, A. Y.-Y., Moulds, S., Murphy, C., Nearing, G.,

575   Shalev, G., Shen, C., Speight, L., Villarini, G., Wilby, R. L., Wood, A., & Zappa, M.

576   (2023). Hybrid forecasting: Blending climate predictions with AI models. *Hydrology*

577   *and Earth System Sciences*, *27*(9), 1865–1889. https://doi.org/10.5194/hess-27-

578   1865-2023

579 Tian, D., He, X., Srivastava, P., & Kalin, L. (2022). A hybrid framework for forecasting monthly

580   reservoir inflow based on machine learning techniques with dynamic climate

581   forecasts, satellite-based data, and climate phenomenon information. *Stochastic*

582   *Environmental Research and Risk Assessment*, *36*(8), 2353–2375.

583   https://doi.org/10.1007/s00477-021-02023-y

584   Tyralis, H., Papacharalampous, G., & Langousis, A. (2019). A Brief Review of Random Forests

585   for Water Scientists and Practitioners and Their Recent History in Water Resources.

586   *Water*, *11*(5), 910. https://doi.org/10.3390/w11050910

587   Wilks, D. S. (2019). Forecast Verification. In *Statistical Methods in the Atmospheric Sciences*

588   (pp. 369–483). Elsevier. https://doi.org/10.1016/B978-0-12-815823-4.00009-2

589   Wood, A. W., Hopson, T., Newman, A., Brekke, L., Arnold, J., & Clark, M. (2016). Quantifying

590   Streamflow Forecast Skill Elasticity to Initial Condition and Climate Prediction Skill.

591   *Journal of Hydrometeorology*, *17*(2), 651–668. https://doi.org/10.1175/JHM-D-14-

592   0213.1

593   Yuan, X., Wood, E. F., & Ma, Z. (2015). A review on climate-model-based seasonal hydrologic

594   forecasting: Physical understanding and system development. *WIREs Water*, *2*(5),

595   523–536. https://doi.org/10.1002/wat2.1088

596